J. King Saud Univ., Vol. 14, *Eng. Sci.* (2), pp. 221-234, Riyadh (A.H. 1422/2002)

Time Series Forecasting Using Wavelet Denoising an Application to Saudi Stock Index

Rumaih M. Alrumaih and Mohammad A. Al-Fawzan
Computer & Electronics Research Institute, King Abdulaziz City for Science and Technology, P.O. Box 6086, Riyadh 11442, Saudi Arabia
E_mail:alrumaih{mfawzan}@kacst.edu.sa

(Received 05 February, 2000; accepted for publication 20 May, 2001)

Abstract. In recent years, wavelet transform has become very popular in many application areas such as physics, engineering, biomedical, signal processing, mathematics, and statistics. In this paper, we present the role of wavelet transform in time series analysis. Saudi Stock Index (SSI) time series was used as a vehicle to highlight the benefits of wavelet transform usage in time series analysis in general and in time series denoising, in particular. SSI was modeled as a deterministic function plus random noise (white or colored). Different denoising techniques were considered with Haar, Daubechies', and Biorthogonal wavelets. Several Forecasting models of SSI were developed for original and denoised series. Namely, Linear Regression (LR), Simple Moving Average (SMA), Exponential Smoothing (ES), Autoregressive (AR), and Autoregressive Moving Average (ARMA). Computational results have shown that more information could be exploited from SSI when it is decomposed into several series with different resolutions using wavelet transform. Moreover, forecasting errors of SSI can be substantially reduced when the index was first denoised using soft thresholding with white noise assumption.

Keywords: Wavelet transform, denoising, forecasting

1. Introduction

Time series forecasting are widely used in many areas such as economics, inventory systems, statistics, etc. There are many forecasting models ranging from basic models such as a simple moving average and linear regression to more advanced models such as autoregressive integrated moving average (ARIMA) and neural networks. These models analyze historical data in order to provide estimates of the future. Time series are not always deterministic series. In fact, most of the time they are considered to be stationary random series. One way to model a time series is to consider it as a deterministic function plus random white or colored noise. When the noise element in a time series is carefully minimized by a process called *denoising*, a better model can be obtained for that series. In order to perform good denoising, mathematical transformations are applied to a series such as Fourier and wavelet transforms.

Wavelet transform [1] decomposes a series into several series with different resolutions. We can think of it as multiresolution analysis because it allows us to look at the original series in a number of different resolutions. Using multiresolution analysis, one can examine the coarse structure "forest" and the fine structure "trees" of a series. In other words, it seems as if one is using a "microscope" to examine the data at different scales or different levels of "magnification". Multiresolution denoising using wavelet transform produces a smoother series yet maintains the fine structure of that series. It proves to be very beneficial to series modeling and forecasting [2,3].

The basic underlying idea of this paper is to present the role of the wavelet transform in time series analysis. Moreover, the study attempts to show the advantages in modeling and forecasting when time series are denoised using wavelet transform. Saudi Stock Index (SSI) was used to carry out the analysis. Two scenarios were considered here, as depicted in Fig. 1. In scenario A, SSI is modeled using one of the following models: Linear Regression (LR), Simple Moving Average (SMA), Exponential Smoothing (ES), Autoregressive (AR), and Autoregressive Moving Average (ARMA). Then, the index is forecasted for each model and forecasting errors were evaluated. While in scenario B, SSI is first modeled as a signal plus random white or colored noise. For both cases, the noise is minimized using different wavelet denoising which are discussed later in this paper. The denoised series are modeled, as in scenario A, and forecasted. Forecasting errors were evaluated and compared to those of scenario A.

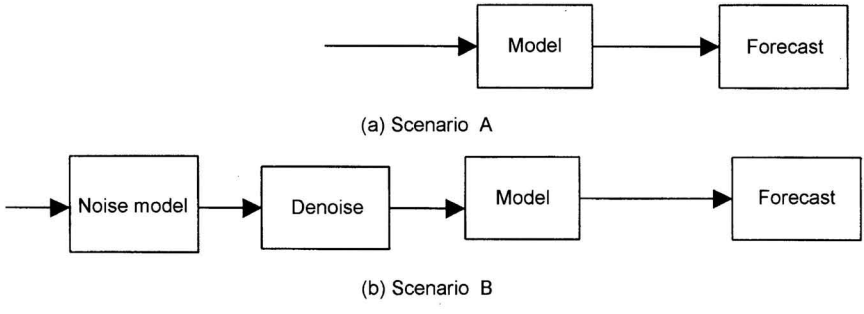

Fig. 1. Modeling scenarios.

This paper is organized as follows, section 2 gives a brief introduction to wavelet transform. Time series denoising using wavelet transform is given in section 3. Section 4 presents computational results with discussion. Finally, conclusions are presented in section 5.

2. The Wavelet Transform

In this section, a brief description of wavelet transform is given. However, excellent references exist in the literature, for example we refer the reader to [4]–[9].

Mathematical transformations are applied to a signal to obtain more information that is not readable in the time domain representation of that signal. Fourier transform, for example, decomposes signals (those satisfying certain conditions) into sum of periodic bases of infinite lengths ($e^{j\omega t} = \cos(\omega t) + j\sin(\omega t)$). It is defined as follows:

$$FT(\omega) = \int_{-\infty}^{+\infty} s(t)e^{-j\omega t}dt \tag{1}$$

where, $FT(\omega)$ is the Fourier transform of the signal *s(t)*. Fourier transform is not localized in time ($FT(\omega)$ is not a function of time), i.e., one can not determine the frequency contents at a specific time instance. Therefore, it is good for signals where frequency content does not change over time. The time-frequency properties of such transform are limited by the *Heisenberg* uncertainty principle:

$$\Delta(t)\Delta(f) \geq \frac{1}{4\pi} \tag{2}$$

where $\Delta(t)$ and $\Delta(f)$ are time and frequency resolutions. The above equation suggests the possibility of trading $\Delta(t)$ for $\Delta(f)$ and vise versa. This is achieved by the well-known short-time Fourier transform (*STFT*), which is an extension of the Fourier transform. It is defined by:

$$STFT(\tau, \omega) = \int s(t)g(t-\tau)e^{-j\omega t}dt \tag{3}$$

where, τ is the shift factor in time and *g(t)* is a window function in time. Short window g(t) improves time resolution at the expense of frequency resolution because short window results in a reduced number of samples, which yields a reduced number of discrete frequencies that can be represented in the frequency domain. The relationship between resolution in time and frequency of the *STFT* is depicted in Figure 2(a).

Similar to Fourier transform, the *STFT* given in (3) can be described as the decomposition of the signal s(t) into the windowed bases function $g(t-\tau)e^{-j\omega t}$. In general, we can write (3) as an inner product of *s(t)* and basis functions $k_{\tau,\omega}(t)$, that is

$$STFT(\tau, \omega) = \int s(t)k_{\tau,\omega}(t)dt \tag{4}$$

note that once a window has been chosen for the *STFT*, then the time-frequency resolution is fixed over the entire time-frequency plane. Therefore, we can have good time resolution or good frequency resolution, but not both. Also, note that the *STFT* is not an orthogonal transform. In fact, the Balian-Low theorem states that there does not exist a smooth window such that the windowed Fourier basis functions are orthogonal and localized in time and frequency [10]. Before we conclude our discussion in Fourier

transform, we need to point out that there exist Fourier-based transforms that are localized in time and frequency such as Smooth Localized Complex Exponential (SLEX) transform, where SLEX basis functions evade the Balian-Low theorem because they are constructed by applying a projection operator, instead of a window, on the Fourier functions (see [10] for details).

Wavelet transform overcomes the resolution limitation of the *STFT* by letting the resolution $\Delta(t)$ and $\Delta(f)$ vary in the time-frequency plane in order to obtain a multiresolution structure. In fact, wavelet transform gives good time resolution (poor frequency resolution) at high frequencies and good frequency resolution (poor time resolution) at low frequencies. Fortunately, most practical signals have high frequency components for short duration and low frequency components for long duration. The relationship between resolution in time and frequency of a wavelet transform is depicted in Fig. 2(b).

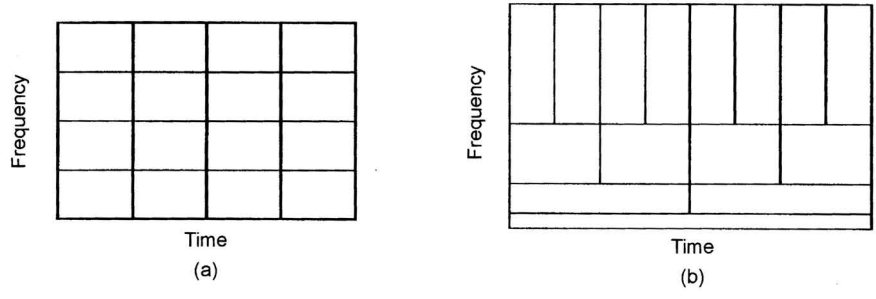

Fig. 2. Time-Frequency resolution plane of (a) Short-Time Fourier Transform, (b) Wavelet Transform.

By replacing ω by the scale variable a and τ by b the wavelet basis are represented by

$$k_{b,a}(t) = \frac{1}{\sqrt{a}} h^*\left(\frac{t-b}{a}\right) \tag{5}$$

and substituting this description in (4) gives the definition of the continuous wavelet transform(*CWT*):

$$CWT(b,a) = \frac{1}{\sqrt{a}} \int s(t) h^*\left(\frac{t-b}{a}\right) dt \tag{6}$$

CWT decomposes the signal s(t) into a weighted set of dilated wavelet function h(t) called the *mother wavelet.* Due to the scaling factor in $h^*\left(\frac{t-b}{a}\right)$, wavelets at high frequencies (smaller scale a) are of limited duration and wavelets at low frequencies (larger scale a) are of longer duration. This varying window structure provides the multi-

resolution time-frequency plane shown in Fig. 2(b). Note that Fourier based transforms are ideal for correlation and spectral estimations. Wavelet based transforms, on the other hand, are intended to estimate the mean structure.

Discrete wavelet transform (*DWT*) is used to decompose discrete sequences. A time-scale representation is obtained using digital filtering techniques. Filters of different cutoff frequencies are used to decompose and analyze the signal at different scales. Frequency resolution of the signal is changed by the filtering operations.

The *DWT* process can be performed by passing the sequence through a half band digital lowpass and highpass filters, to be called $h[n]$ and $g[n]$, respectively. By doing so, frequency resolution is doubled because only half of the original band exists in the filtered sequences. After passing the sequences through the filters, half of the samples can be eliminated according to the Nyquist's criterion (i.e., half of the samples are redundant). Therefore, after subsampling by two, the time resolution is reduced by half. The above procedure can be repeated for further decomposition. Figure 3 illustrates this process for 3-level decomposition, where s is the original sequence, h[n] and g[n]are lowpass and highpass analysis filters, and D^1 is the first-level discrete wavelet coefficients (DWC), D^2 is the second-level DWC , D^3 and A^3 are the third-level DWC . rh[n] and rg[n] are lowpass and highpass synthesis filters. Note that the original sequence s can be synthesized by the low and high frequencies sequences, i.e., s = a3+d3+d2+d1.

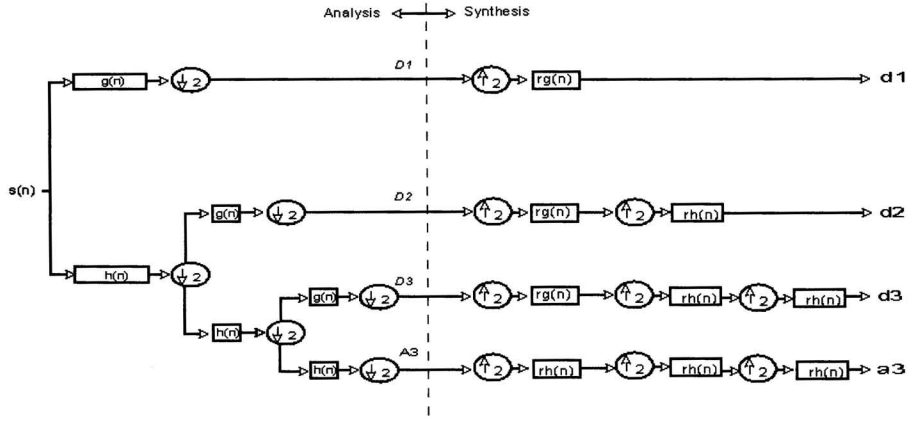

Fig. 3. Analysis-synthesis block diagram for the discrete wavelet transform.

Orthogonal wavelets such as Haar, Daubechies', and Coifman wavelets, h[n], g[n], rh[n], and rg[n] are related as follows [4]:

$$g[n] = (-1)^n h[N-n], \forall n \in \{0,1,2,\ldots, N-1\} \quad (7)$$

$$rh[n] = 2h[n], \forall n \in \{0,1,2,\ldots, N-1\} \quad (8)$$

$$rg[n] = -2(-1)^n h[n], \forall n \in \{0,1,2,\ldots, N-1\} \quad (9)$$

where, N is the order of the filter.

While for Biorthogonal wavelets, h[n], g[n], rh[n], and rg[n] are related as follows [5]:

$$g[n] = (-1)^n rh[1-n], \forall n \in \{0,1,2,\ldots, N_1-1\} \quad (10)$$

$$rg[n] = 2h[1-n], \forall n \in \{0,1,2,\ldots, N_2-1\} \quad (11)$$

where N_1 and N_2 are the order the filters.

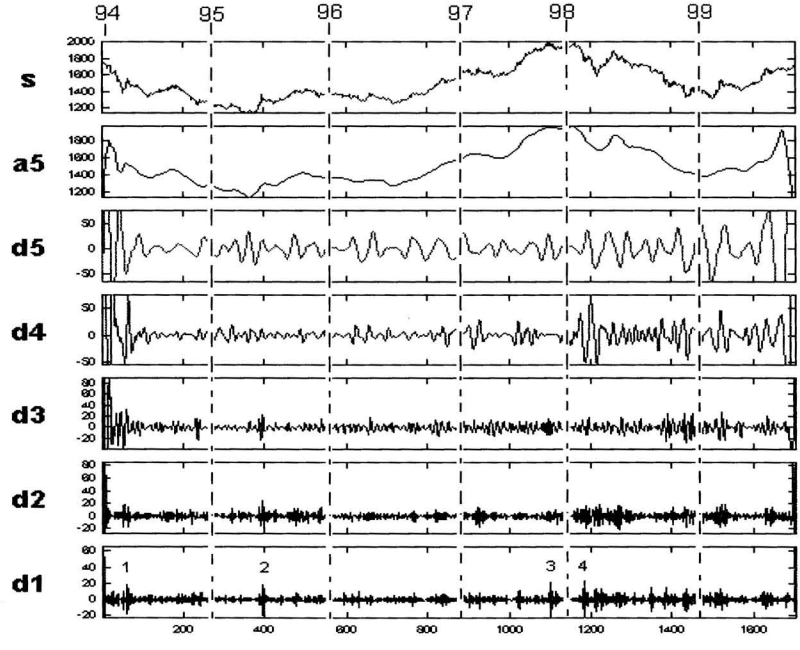

Fig. 4: 5-level wavelet transform for the daily SSI using daubechies' filter of order four (*N*=4).

Figure 4 shows a five-level multiresolution wavelet synthesis of the daily SSI series for 1705 days starting from January 26, 1994 until November 4, 1999 using Daubechies' wavelet of order four (the order of the filters N=4). The coarse structure a5 shows the market trend, i.e., the overall picture "forest". Let us zoom in and examine d5, we can see that there was irregular behavior in early 1994, mid 1995, and all of 1998–1999. If we zoom in a little more and examine d4, the time resolution increases and we can see more clearly the 1994 and 1998 market decline. Finally, if we use the best lens we have and examine d1, we can see the market behavior almost daily, where we can see the sharp decline of April 14, 1994, October 28, 1997, and March 18, 1998 (points number 1,3, and 4 in d1 plot of figure 3) and the sharp increase of June 21, 1995 (point number 2 in d1 plot of Fig. 3). We can also see that the market was smooth and stable during the period between July 1995 until October 1997 (between points 2 and 3 in d1 plot of Figure 4). Note that due to boundary decomposition problem of the wavelet transform, one should disregard the very beginning and the very end of the decomposition series a5, d5, d4, d3, d2, and d1.

3. Time Series Denoising Using Wavelet Transform

Conceptually, wavelet coefficients correspond to details and when details are small, they could be considered as noise and therefore omitted without compromising the sharp detail of the original series (unlike the Fourier transform). In other words, without going through a formal mathematical argument, wavelet transform compresses most of the energy of the original series into a small number of large wavelet coefficients. Thus, the few wavelet coefficients representing the original series stick up above the noise. Therefore, the thresholding has the effect that it kills the noise while not killing the series. This is the beauty of wavelet transform. Hence, the idea behind wavelet denoising is to threshold the wavelet coefficients at every multiresolution level (in some manner) to clean out unimportant details considered to be noise.

The underlying model for the noisy series is basically of the following form:

$$S_t = f_t + e_t \tag{12}$$

where

e_t is a multivariate normal distribution process with mean zero and covariance matrix Γ_t.

The denoising objective is to suppress the noise part of the series S_t and to recover f_t.

Wavelet transform has a 'decorrelating' feature. Since the mapping from the original series to the wavelet coefficients on any level is essentially a band-pass filter, there will tend to be little or no correlation between the wavelet coefficients at different levels [11]. Hence, for each level j we will have a threshold λ_j. Three thresholding techniques were considered here, namely:

(i) *Universal thresholding*
Threshold is given by the following formula [12]

$$\lambda_j = \sigma_j \sqrt{\frac{2\log n}{n}} \tag{13}$$

where σ_j is an estimate of the variation of wavelet coefficients of level j, and n is the number of wavelet coefficients in that level.

(ii) *SURE thresholding*
Threshold was selected based on the Stein's Unbiased Risk Estimate (SURE). Details are given in [11].

(iii) *Minimax thresholding*
The threshold was found using the Minimax principle. This fixed threshold is chosen to yield Minimax performance for mean square error against an ideal procedure. The Minimax principle [13] is used in statistic in order to design estimators. Since the denoising signal can be assimilated to the estimator of the unknown regression function, the Minimax estimator is the option that realizes the minimum of the maximum mean square error obtained for the worst function in a given set.
Noise $e_t$was considered to be (a) *white* or (b) *colored.*

After estimating the threshold of a level j, wavelet coefficients of that level are either hard or soft thresholded. Hard thresholding is keep or kill policy. Meaning that if a wavelet coefficient is less than the threshold it would be set to zero, otherwise it stays unchanged. On the other hand, soft thresholding shrinks all nonzero coefficients towards zero, which gives a smooth denoising series. Wavelet coefficients are soft thresholded by

$$d_{j,k}^{soft} = \begin{cases} \text{sgn}(d_{j,k})(|d_{j,k}| - \lambda_j) & \text{if } d_{j,k} \geq \lambda_j \\ 0 & \text{if } d_{j,k} < \lambda_j \end{cases} \tag{14}$$

where $d_{j,k}$ is the k^{th} wavelet coefficient in the j^{th} level, and λ_j is the threshold of that level. It was shown in [14] that soft thresholding outperformed hard thresholding for modeling and forecasting SSI. Therefore, here we only consider soft thresholding.

4. Results and Discussions

As mentioned in the introduction and depicted in Fig. 1, we considered two different scenarios.

Scenario A:
The daily SSI was modeled using the models mentioned below. Then, the index was forecasted for each model and forecasting errors were evaluated.

Scenario B:

The daily SSI noise model was considered to be either white or colored. For both cases, the index was denoised using thresholding techniques mentioned in section 4 with wavelet families given below. Then, the denoised series were modeled, using the models mentioned below, and forecasted. Forecasting errors were evaluated and compared to those of scenario A.

Scenarios A and B were applied in 1705 data points of the SSI starting from January 26, 1994 until November 4, 1999. The first 1200 points were used for estimation and the last 505 points were used for forecasting. The actual stock index values for these periods are available. This enables us to evaluate the performance measures for all forecasting models. The forecasting models used are as follows:

1. LR: Linear Regression
2. SMA: Simple Moving Average with the number of values included in the average M=4
3. ES: Exponential Smoothing with the smoothing factor $\alpha = 0.01$
4. AR(2): Autoregressive with two-step regression $p = 2$.
5. ARMA(2,4): Autoregressive Moving Average with two-step regression and four-step moving average $p = 2$ and $q = 4$.

The above parameters were selected after careful modeling and fitting (*Eviews* version 3 software was used for modeling). The performance measures used in the analysis are Root Mean Squared Error (RMSE) and Mean Absolute Deviation (MAD). RMSE and MAD are computed as follows.

$$RMSE = \sqrt{\frac{\sum_{i=1}^{n}(x_i - fr_i)^2}{n}} \tag{15}$$

$$MAD = \sqrt{\frac{\sum_{i=1}^{n}|x_i - fr_1|}{n}} \tag{16}$$

where x_i and fr_i are the actual and forecasted value for period *i*.

In the denoising block of scenario B, Three different wavelet families were used. They are:

1. Haar wavelet with 5-multiresolution levels.
2. Daubechies wavelet of order 4 and 5-multiresolution levels
3. Biorthogonal wavelet of order 3 and 3 and 5-multiresolution levels.

For each selected wavelet, SSI was first analyzed to five multi-resolution levels. Then, each level was denoised using (i) Universal, (ii) SURE, and (iii) *Minimax thresholding*. This process was repeated twice. One for white noise assumption and the other for colored noise assumption.

Tables 1-3 summarize the performance measures for the different models of the original and denoised SSI using Universal, Minimax, and Sure thresholding with white noise assumption. In appendix A, we report the results when the noise is assumed to be colored. Several observations are in order here. First, one may note that the best estimation models for the original index can be arranged in an increasing order as follows:

ARMA(2,4), AR(2), SMA, ES, and LR. Second, we can observe that wavelet denoising does not help much when simple models were used, i.e., LR, SMA, and ES. However, when AR and ARMA models were used wavelet denoising reduces forecasting errors. The reduction is maximum when the index was Universally thresholded using Biorthognal wavelet (note from Table 1 the good reduction in RMSE and MAD of AR(2) from 11.7 to 8.34 and from 8.6 to 6.15, respectively). Finally, from Tables 1–3 and Tables 1A-3A in the appendix, one can observe that colored noise assumption is not suitable at all for SSI modeling, rather the noise in Saudi stock index is more likely to be white. Incidentally, in [15] we have shown that the noise in the NASDAQ-100 index is colored.

Table 1. RMSE & MAD for various forecasting models of SSI versus thedenoised index using Universal thresholding with white noise assumption

Model	Original		Daubechies		Haar		Biorthogonal	
	RMSE	MAD	RMSE	MAD	RMSE	MAD	RMSE	MAD
LR	295.1	252.4	294.8	252.2	294.2	251.4	296.4	254.8
SMA	18.9	14.0	18.43	13.42	18.4	13.1	18.33	13.36
ES	58.3	43.7	56.6	42.7	55.7	42.1	57.5	43.5
AR(2)	**11.7**	**8.6**	9.14	6.92	13.9	10.39	**8.34**	**6.15**
ARMA(2,4)	11.65	8.6	9.12	6.9	13.9	10.32	8.34	6.15

Table 2. RMSE & MAD for various forecasting models of SSI versus thedenoised index using soft Minimax thresholding with white noise assumption

Model	Original		Daubechies		Haar		Biorthogonal	
	RMSE	MAD	RMSE	MAD	RMSE	MAD	RMSE	MAD
LR	295.1	252.4	295.03	252.33	294.95	252.26	295.13	252.42
SMA	18.9	14.0	18.38	13.44	18.14	13.01	18.44	13.50
ES	58.3	43.7	58.35	43.70	58.43	43.66	58.36	43.68
AR(2)	11.7	8.6	9.06	6.65	11.89	8.64	8.87	6.33
ARMA(2,4)	**11.65**	**8.6**	9.01	6.64	11.42	8.36	**8.78**	**6.28**

Table 3. RMSE & MAD for various forecasting models of SSI versus the denoised index using soft SURE thresholding with white noise assumption

Model	Original		Daubechies		Haar		Biorthogonal	
	RMSE	MAD	RMSE	MAD	RMSE	MAD	RMSE	MAD
LR	295.1	252.4	295.09	252.39	295.09	252.38	295.09	252.39
SMA	18.9	14.0	18.81	13.88	18.58	13.59	18.86	13.92
ES	58.3	43.7	58.33	43.67	58.35	43.68	58.33	43.67
AR(2)	**11.7**	**8.6**	**10.18**	7.37	10.59	**7.28**	10.57	7.70
ARMA(2,4)	11.65	8.6	10.25	7.41	10.52	7.28	10.65	7.70

It is worth mentioning here that there is no clear-cut answer as to why these wavelet families were selected in particular among many other families. Wavelet denoising is a data dependent process. However, Haar wavelet is a very basic wavelet family and it is presented here for comparison purposes. Moreover, after many experimental trials with many wavelet families, it was found that Daubechies and Biorthogonal wavelets outperform the other families in terms of denoising the Saudi stock index.

5. Conclusion

In this paper, we used the Saudi stock index, as an example, to show the benefits of using wavelet transform in time series analysis. It was shown here that more information could be exploited from a series when it is decomposed into several series with different resolutions using wavelet transform. Moreover, computational results have shown that the noise in the Saudi stock index is more likely to be white and when it is carefully minimized using wavelet denoising, then forecasting errors can be substantially reduced.

References

[1] Rioul, O. and Vetterli, M. "Wavelets and Signal Processing". *IEEE SP Magazine*, (Oct. 1991), 14-38.

[2] Lee, G. "Wavelets and Wavelet Estimation: A Review". *Journal of Economics Theory and Econometrics*, 4, No. 1 (1998), 123-157.

[3] Arino, M. and Vidakovic, B. "On Wavelet Scalograms and Their Applications in Economic Time Series". *Discussion paper* 95-30, ISDS, Duke University, 1995.

[4] Daubechies, I. *Ten Lectures on Wavelets*, Society for Industrial and Applied Mathematics, 1992.

[5] Burrus, C.S., Gopinath, R. and Guo, H. *Introduction to Wavelet and Wavelet Transforms, a Primer*, Prentice Hall, 1998.

[6] Kaiser, G. *A Friendly Guide to Wavelets*, Bikhauser, 1994.

[7] Chui, C.K. *Wavelets: A Tutorial in Theory and Applications*, Academic, 1992.

[8] Akansu A.N. and Haddad, R.A. *Multiresolution Signal Decomposition Transforms, Subbands and Wavelets*, Academic, 1992.

[9] Bentley, P.M. and Mcdonnell, J.T.E. "Wavelet Transform an Introduction". *Electronics & Communication Engineering Journal*, (Aug. 1994), 175-186.

[10] Wickerhauser, M. "Adapted Wavelet Analysis from Theory to Software". *IEEE Press*, Wellesely, MA., 1994.

[11] Johnstone, I. and Silverman, B. W. "Wavelet Thresholding Estimators for Data with Correlated Noise". *Journal of Roy. Stat. Soc.*, Series B, 59 (1997), 319-351.

[12] Donoho, D. and Johnstone, I. "Ideal Spatial Adaptation by Wavelet Shrinkage". *Biometrica,* 81 (1994), 425-455.

[13] Donoho, D. and Johnstone, I. "Adapting to Uunknown Smoothing via Wavelet Shrinkage". *J. Amer. Statist. Association,* 90 (1993), 1200-1224. ,

[14] Alrumaih, R.M. and Al-Fawzan, M.A. "Time Series Analysis Using Wavelet Transform". *16th National Computer Conference*, 4-7 February 2001, Riyadh, Saudi Arabia.

[15] Alrumaih, R., Al-Fawzan, M., Lam, K.P. and Ng, H.S. "Application of Wavelet Denoising Techniques To Financial Time Series Forecasting". *Conf. on Info. Sys.* (SCI'2001), Orlando, USA, July 22-25, 2001.

Appendix A

Computational results for the colored noise assumption are given here:

Table 1A. RMSE & MAD for various forecasting models of SSI versus the denoised index using *Universal* thresholding with colored noise assumption

Model	Original		Daubechies		Haar		Biorthogonal	
	RMSE	MAD	RMSE	MAD	RMSE	MAD	RMSE	MAD
LR	295.1	252.4	295.79	253.03	292.04	249.57	293.69	251.0
SMA	18.9	14.0	42.85	31.07	41.65	29.15	38.32	27.86
ES	58.3	43.7	61.18	45.33	59.18	43.23	59.84	43.24
AR(2)	**11.7**	**8.6**	41.83	30.05	42.85	30.04	38.09	27.90
ARMA(2,4)	11.65	8.6	41.95	30.07	43.02	30.14	38.52	28.13

Table 2A. RMSE & MAD for various forecasting models of SSI versus the denoised index using *Minimax* thresholding with colored noise assumption

Model	Original		Daubechies		Haar		Biorthogonal	
	RMSE	MAD	RMSE	MAD	RMSE	MAD	RMSE	MAD
LR	295.1	252.4	295.03	252.32	292.04	249.57	294.02	251.4
SMA	18.9	14.0	36.14	27.88	37.80	27.80	33.12	25.06
ES	58.3	43.7	60.13	44.52	58.61	42.97	59.35	42.85
AR(2)	**11.7**	**8.6**	34.35	26.50	38.01	28.14	32.35	24.64
ARMA(2,4)	11.65	8.6	34.55	26.72	38.12	28.21	32.60	24.83

Table 3A. RMSE & MAD for various forecasting models of SSI versus thedenoised index using SURE thresholding with colored noise assumption

Model	Original		Daubechies		Haar		Biorthogonal	
	RMSE	MAD	RMSE	MAD	RMSE	MAD	RMSE	MAD
LR	295.1	252.4	294.45	251.8	292.04	249.57	294.86	252.17
SMA	18.9	14.0	28.35	22.23	34.45	26.43	26.81	20.12
ES	58.3	43.7	59.12	43.95	57.96	42.68	58.85	42.80
AR(2)	**11.7**	**8.6**	24.69	19.88	33.44	26.70	25.03	19.32
ARMA(2,4)	11.65	8.6	24.90	20.06	33.46	26.71	25.18	19.48